Spring 5-2016

Dynamic Modeling of a Catamaran Using a Lagrangian Approach

Tamara R. Thomson

DYNAMIC MODELING OF A CATAMARAN USING A LAGRANGIAN APPROACH

by

Tamara R. Thomson

A Thesis Submitted in Partial Fulfillment
of the Requirements for a Degree with Honors
(Mechanical Engineering)

The Honors College

University of Maine

May 2016

Advisory Committee:

Michael “Mick” Peterson, Professor of Mechanical Engineering
Sergey Lvin, PhD, Lecturer of Mathematics
Margaret O. Killinger, PhD, Associate Professor and Rezendes Preceptor for the Arts
Murray Callaway, Lecturer of English
Zhihe Jin, PhD, Associate Professor of Mechanical Engineering

Abstract

In this thesis, the development and application of a dynamic model of the 2016 Autonomous Boat Team's catamaran are discussed. The model is two dimensional and describes the motion of the boat in a calm freshwater environment. The linear and rotational equations of motion used in the model were derived by employing Lagrangian dynamics, and the thrust of the motors and drag of the hulls were found through experimentation. The resulting equations are $ma = \frac{1}{2} \cdot \rho \cdot \dot{x}^2 C_{Df} A + 2F$ and $I\alpha = \frac{b}{16} \cdot \rho \cdot \dot{\theta}^2 C_{Dr} A + F_2 \cdot \frac{b}{2} - F_1 \cdot \frac{b}{2}$. The thrust and drag here vary with respect to voltage and velocity.

The following document is organized to first supply the reader with background information sufficient to understand the project's purpose and merits and then discuss the experiments and derivations necessary for completing the objectives. Next, the resulting model is presented and discussed at length followed by a section about the applications and future work suggestions for this project.

This thesis is dedicated to my family, Stacy, Randall, and

Anthony Thomson.

Acknowledgements

I would like to acknowledge the contributions made by my entire thesis committee, most notably Dr. Mick Peterson, my thesis advisor. Thank you for all the help and support you've given me throughout my undergraduate experience.

Additionally, I'd like to acknowledge the work contributed by my capstone team that was critical for the completion of this thesis. Riley Mattor, Chris Derr, and Ben Dickinson were extremely helpful and surprisingly willing to assist me at every stage of this project. Thank you.

Table of Contents

Table of Figures

Introduction

This thesis describes the efforts employed in the development of a model to predict the movement of a catamaran in a calm freshwater environment and displays the results. To help reader understand the scope of the undertaking this was, the thesis begins with a description of the catamaran in question. The catamaran whose motion is described with this model is the 2016 Autonomous Boat Team's capstone project. It is 16.5 feet in length and 8.5 feet wide, measured from the points of the pontoons. The catamaran is driven by two Minn Kota trolling motors (model number C2 30) attached directly behind the pontoons. A labeled diagram of the catamaran is displayed below in Figure 1.

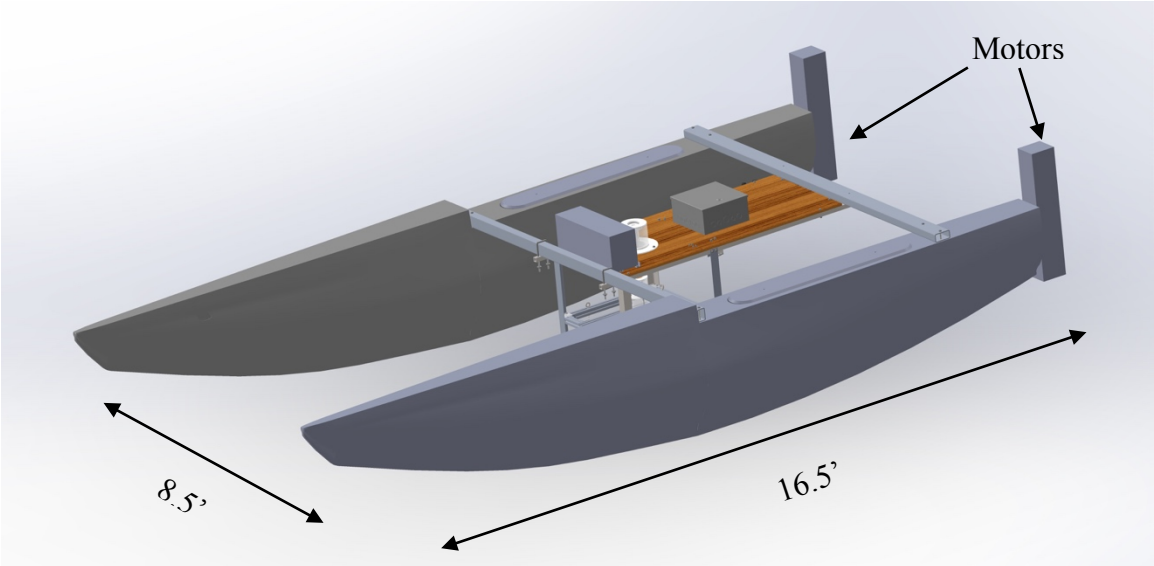

Figure 1 SolidWorks diagram of catamaran

Objectives

The overall objective of this undertaking was to create a dynamic model of a catamaran. In order to complete this model, several intermediate objectives had to be met. Those objectives are listed below.

- Analytically determine the equations of motion for the catamaran using Lagrangian dynamics.
- Experimentally determine the drag coefficient associated with the catamaran in fresh water.
- Create thrust curves for the motors using experimental data.
- Determine the moment of inertia of the catamaran using a SolidWorks model.

Each of the objectives listed above was essential for the completion of the model. Without accurately measured criteria, the model would be inaccurate, and without correctly derived equations of motion, even the most accurate experimental data is moot.

Scope of Project

This thesis is a portion of a larger capstone project that was undertaken simultaneously by the 2016 Autonomous Boat Team. In order to clarify the value of completing a dynamic model of the catamaran, it is necessary to explain the background of the capstone project itself.

Hydroelectric energy is the largest form of renewable energy in the United States, providing approximately 96% of the renewable energy consumed by our country in 2005 [1]. New sources of hydroelectric energy are continually being sought. Generators placed in dams are reliable and effective energy sources, but damming flowing water is not always a viable option in populated or protected regions.

The ocean presents an enormous amount of harnessable energy in its tides. Unlike sources of solar and wind energy, tidal energy is very dependable; the tides operate on reliable schedules all year long. It is widely known that the tides are largely caused by the gravitational attraction between the earth and the moon, meaning that tidal energy cannot be overdrawn and will not fail.

Maine has some of the largest tidal ranges in the world. The highest recorded on earth are in the Bay of Fundy which is located in the Gulf of Maine. Here, the tidal range reaches up to 50 feet [2]. Tidal ranges such as this are uncommon, but other areas on the coast of Maine have relatively high tidal ranges as well. The tidal range in Cobscook Bay, a shallow estuary in Downeast Maine, averages 24 feet [3], which is much smaller than that of the Bay of Fundy, but is eight time the average world-wide [2]. Bays with high tidal ranges produce large currents, providing the potential for collection of large amounts of energy. Ocean Renewable Power Company (ORPC) recognized this potential and developed and installed a tidal turbine in Cobscook Bay. However, several factors had to be considered before installation was possible.

The Cobscook Bay area is home to about 7,000 people, many of whom are fishermen that depend on the health of the fishery for their livelihoods [3]. The population of fish is not only crucial to the inhabitants in the area. It is also vital to the fragile ecosystem in Cobscook Bay and the entire Gulf of Maine that the fish remain unharmed. As Michael Johnson writes,

> The area is home to important fish species such as Atlantic herring, winter flounder, Atlantic cod, and haddock, as well as anadromous fish including alewife, blueback herring, and rainbow smelt. These anadromous fish live within the Cobscook Bay estuary until they reach maturity, and then make annual spawning migrations into the freshwater rivers and streams that flow into the bay. They serve as food for larger species, including Atlantic cod, haddock, bluefin tuna, bluefish, sea birds, and marine mammals like seals. Cobscook Bay is also a vital center for Maine's aquaculture because it provides prime habitat for sea scallops, sea urchins, and soft-shelled clams.
>
> [3]

Such valuable ecological resources need to be protected both for the good of the local economy and the environment. Understanding this, ORPC placed in Cobscook Bay a platform designed by the Northeastern Regional Association of Coastal Ocean Observing Systems (NERACOOS), equipped with hydro-acoustic sensors to monitor the movements and migration patterns of the indigenous community of fish. The goal was to collect data to determine if a turbine could be installed without harming wildlife in the bay. More specifically, the intent was to determine if the installation would negatively impact the population of fish. Activity in the area directly around the NERACOOS platform would compare multi-year base line data with data obtained after the installation of ORPC's turbine. An adaptive management plan would then require mitigation of the impact or even removal of the turbine if its effects were excessive. The data set required for this effort is significant because because of the influence of annual variations in the fish population. The cost and complexity of this monitoring is a significant barrier to the adoption of tidal energy generation. The large amount of hydro-acoustic data obtained from the monitoring would require large amounts of data to be obtained over long periods of time.

The goal of the 2016 Autonomous Boat Team's capstone project was to design, build, and program a prototype of a boat that could autonomously navigate to the GPS coordinates of the NERACOOS platform and make a physical connection with an offshoot buoy, collecting the data and providing power when necessary. The physical connection was essential because of the large amounts of data being collected by the hydro-acoustic sensors weekly – several terabytes. It is also essential because the boat is intended to help recharge the batteries to supply the high power demand of the platform. This is especially necessary during periods of the year when solar power is limited. The completion of this boat would provide relief for workers collecting data year round. This would also significantly reduce the cost of collecting the data from the offshore platform.

Any vehicle is difficult to automate, and this catamaran was no exception. It was essential to understand how the catamaran reacted when voltage was supplied to its motors so it could be programmed to navigate to the NERACOOS platform unmanned. The model created for the completion of this thesis was designed to describe the motion of the boat in calm water, which is a stepping stone to the creation of a model that would describe the motion of the catamaran at sea, with applied waves and currents. The model described here was implemented in the catamaran prototype which was merely a proof of concept never intended to be operated in choppy water or without supervision.

Dynamics – History and Options

Dynamics is the study of moving bodies. Lagrangian mechanics has been employed to create the model presented in this thesis. In an effort to shed some light on

the decision to use Lagrangian mechanics, a brief explanation of the development of Newtonian and Lagrangian dynamics will be provided in this section.

As Sir Isaac Newton said in the preface to the *Principia*, "mechanics will be the science of motion resulting from any forces whatsoever, and of the forces required to produce any motion" [4]. This quote gives the reader an idea of the breadth and value of dynamics.

Newton is the father of Newtonian dynamics, also called vectorial mechanics and the direct approach, which is commonly taught in undergraduate classrooms today. Newtonian dynamics relies on Newton's famous three laws. Jakob Bernoulli later discovered that solutions to dynamic problems could be solved for by balancing forces and moments. It was Euler who first recognized and wrote these equations: $F_x = ma_x$, $F_y = ma_y$, $F_z = ma_z$. Later, Euler discovered and published his First and Second Axioms, which defined linear and angular momentum. With this advancement, finally classical mechanics was born, and it has changed very little since 1776 [5].

Another approach based on energy and work exists, Lagrangian dynamics. This approach is also called the indirect approach and analytical dynamics. Famous German mathematician and philosopher Gottfried Leibniz was the first recorded believer in the indirect method. In the 1600's Leibniz theorized that there were "living" and "dead" forces, and he believed that changes in these forces could be related to work done in a system. Nearly two centuries later, Lagrange and Euler studied the principle of least

action and developed hypotheses about kinetic and potential energy. In 1788, Lagrange published *Mecanique Analytique*, giving birth to Lagrangian mechanics [5].

The histories of these two methods are enlightening. They outline the work that went into their development and touch on some important aspects of the two methods that should be considered before deciding which is best applied to certain systems. Both approaches generate the same answers, but more steps are often required for problem solving in Newtonian mechanics. Newtonian mechanics is a more intuitive process; the effects of forces and moments can be observed. Energy, on the other hand, is a nebulous concept until it is fully grasped. The beauty of this indirect method, though, is that all components are scalar, giving Lagrangian mechanics the hefty advantage of having generalized coordinates. No matter how the coordinates of a system are oriented or how they change, Lagrange's methods do not vary. It is for this reason that Lagrangian dynamics was selected for derivation of this model. In this case the combined angular and linear motion of the boat is easily combined into two equations of motion.

Methods and Analysis

This thesis combines analysis and experimental testing. Finding the equations of motion of the catamaran required an analytical derivation using Lagrangian dynamics. The thrust curves of the engines were then found experimentally, as was the drag force on the boat. The coefficient of drag,

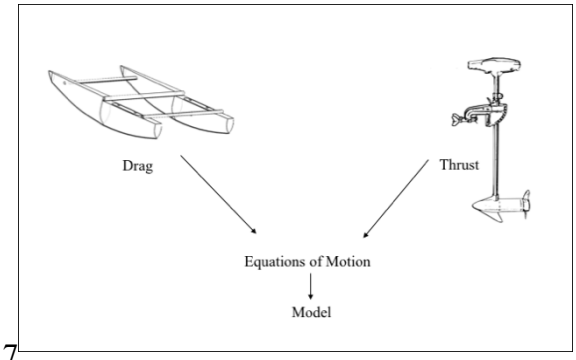

Figure 2 Flowchart of inputs for model

necessary to predict the drag induced by traveling at a range of velocities, was then found from additional analysis. Figure 3 shows a schematic flowchart of the experimental and analytical results and how they relate to the model. The process by which each of these components were developed is outlined in the following sections of the document.

Derivation of the Equations of Derivation of the Equations of Motion

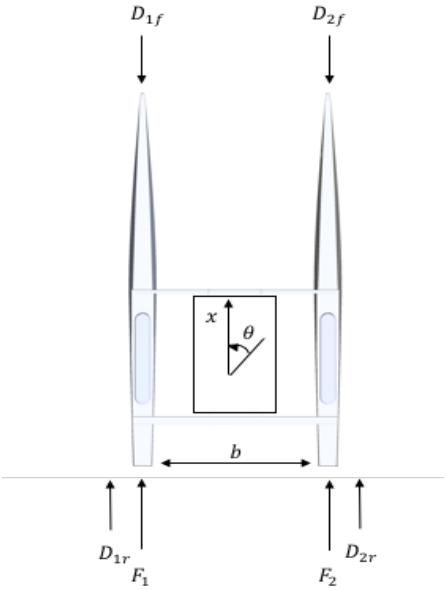

Figure 3 FBD of catamaran

The application of a Lagrangian formulation of the equations of motion using linear and rotational terms was relatively simple. The methodology was easily able to address the complexities of the problem. This thesis work included learning how to derive the equations of motion using a Lagrangian method which is not a part of the undergraduate engineering curriculum at UMaine. It was necessary to build a foundation of knowledge of the process with less complex problems prior to tackling this one. This previous study provided a clear understanding of the proper steps necessary to complete the derivation of the equations of motion. Before analysis began, a free body diagram (FBD) of the system was drawn (Figure 3).

To complete this solution, the steps in *Fundamentals of Applied Dynamics* were followed [6]. The first step in this process was to define the generalized coordinates used in the system. This is done below.

$$\xi_i = x, \theta \qquad \partial\xi = \partial x, \partial\theta$$

The next step is to define generalized forces. The system analyzed here, the catamaran, does not include any conservative forces. The generalized forces nonconservative work is

$$\partial W|^{nc} = \frac{b}{2}(\partial\theta)(D_r) + F_2(\partial x)\left(\frac{b}{2}\right)D_{2r} - (F_1)(\partial x)\left(\frac{b}{2}\right)D_{1r} + (F_1 + F_2)\partial x \qquad \text{(Eq. 1)}$$

where $W|^{nc}$ is the nonconservative work completed by the forces acting on the catamaran. The rotational coordinate is θ, and x is the translational coordinate. The distance between the pontoons is b. D_{2r} is the force of drag induced by pontoon two moving backward, and D_{1f} is the force of drag induced by pontoon one moving forward. The entire drag induced when the boat is turning is $D_r = \frac{1}{2}(D_{2r} + D_{1f})$. Thrust of the motors is represented by F_1 and F_2, respectively.

The equation for drag (Equation 2) is commonplace and can be referenced from any fluid mechanics book. The author references *Fundamentals of Fluid Mechanics* [7].

$$D_r = \frac{1}{2}\rho \cdot V^2 \cdot C_D \cdot A \qquad \text{(Eq. 2)}$$

In Equation 2, ρ is the density of water, $65.55\,\frac{1bm}{ft^3}$ [7], V is the velocity of the catamaran, C_D is the drag coefficient of the pontoons, and A is the cross-sectional area of the pontoons.

The drag equation can be expanded by elaborating on velocity.

$$D_r = \frac{1}{2}\rho \cdot (\frac{b}{2}\dot{\theta})^2 \cdot C_D \cdot A \qquad \text{(Eq. 3)}$$

Inserting Equation 3 into Equation 1 yields Equation 4.

$$\partial W|^{nc} = \frac{b}{2}(\partial\theta)\left(\frac{1}{2}\rho \cdot \left(\frac{b}{2}\dot{\theta}\right)^2 \cdot C_D \cdot A\right) + F_2(\partial x)\left(\frac{b}{2}\right)D_{2r} -$$

$$(F_1)(\partial x)(\tfrac{b}{2})D_{1r} + (F_1 + F_2)\partial x \qquad \text{(Eq. 4)}$$

The next step outlined by Williams is to define the Lagrangian term. The Lagrangian is defined as the kinetic energy of a system, T, minus the potential, U. For this application, there is no potential energy. Therefore, $U = 0$. The kinetic energy of this system is shown in Equation 5.

$$T = \frac{1}{2} \cdot I \cdot \dot{\theta}^2 + \frac{1}{2} m \cdot \dot{x}^2 \qquad \text{(Eq. 5)}$$

I is the moment of inertia, $\dot{\theta}$ is the rotational velocity, m is the mass of the catamaran, and $\dot{x}$ is the linear velocity.

The resulting Lagrangian then is the kinetic energy of the system. This is shown in Equation 6.

$$\mathcal{L} = \frac{1}{2} \cdot I \cdot \dot{\theta}^2 + \frac{1}{2} m \cdot \dot{x}^2 \qquad \text{(Eq. 6)}$$

Next is step four, employing Lagrange's equation. Lagrange's equation is seen below in Equation 7.

$$\frac{d}{dt}\frac{\partial \mathcal{L}}{\partial \dot{\xi}_i} + \frac{\partial \mathcal{L}}{\partial \xi_i} = \Xi_i \qquad \text{(Eq. 7)}$$

Remembering back to the generalized coordinate definitions, $\partial\xi = \partial x, \partial\theta$. Now, Lagrange's equation can be evaluated for the two generalized coordinates of this system.

$$\frac{d}{dt}\frac{\partial \mathcal{L}}{\partial \dot{x}} + \frac{\partial \mathcal{L}}{\partial x} = \Xi_x = m\ddot{x} = \frac{1}{2} \cdot \rho \cdot \dot{x}^2 C_{Df} A + 2F \qquad \text{(Eq. 8)}$$

$$\frac{d}{dt}\frac{\partial \mathcal{L}}{\partial \dot{\theta}} + \frac{\partial \mathcal{L}}{\partial \theta} = \Xi_\theta = I\ddot{\theta} = \frac{b}{16} \cdot \rho \cdot \dot{\theta}^2 C_{Dr} A + F_2 \cdot \frac{b}{2} - F_1 \cdot \frac{b}{2} \qquad \text{(Eq. 9)}$$

The partial derivative of nonconservative work can be defined as shown in Equation 10.

$$\partial W|^{nc} = \Xi_x \cdot \partial x + \Xi_\theta \cdot \partial\theta \quad \text{(Eq. 10)}$$

Expanding by inserting Ξ_x and Ξ_θ yields Equation 11.

$$\partial W|^{nc} = (\tfrac{1}{2} \cdot \rho \cdot \dot{x}^2 C_{Df} A + 2F) \cdot \partial x + (\tfrac{b}{16} \cdot \rho \cdot \dot{\theta}^2 C_{Dr} A + F_2 \cdot \tfrac{b}{2} - F_1 \cdot \tfrac{b}{2}) \cdot \partial\theta \quad \text{(Eq. 11)}$$

Since $\ddot{x}$ is linear acceleration, and $\ddot{\theta}$ is angular acceleration, the translational and rotational components can be rewritten:

$$ma = \tfrac{1}{2} \cdot \rho \cdot \dot{x}^2 C_{Df} A + 2F \quad \text{(Eq. 12)}$$

$$I\alpha = \tfrac{b}{16} \cdot \rho \cdot \dot{\theta}^2 C_{Dr} A + F_2 \cdot \tfrac{b}{2} - F_1 \cdot \tfrac{b}{2} \quad \text{(Eq. 13)}$$

Equation 12 and 13 are the equations of motion which describe the system.

Conducting the Drag Experiment

There are several kinds of drag: form drag, pressure drag, and frictional drag. For the purposes of this project, all significant forms of drag were lumped together to create one drag term that could be measured.

To find the drag force on the catamaran, the catamaran was launched in a body of water and tied behind another boat. A spring scale was attached in line between the catamaran and the towing boat in such a way as to allow for a member of the group to collect measurements from it. A GPS was located on the towing boat and was used to collect the speed of the two crafts during the experiment. A diagram of the testing setup is included below in Figure 4 for clarity.

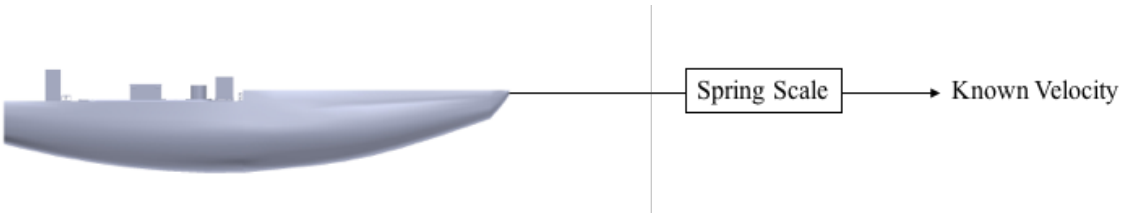

Figure 2 Diagram of drag testing setup

Before testing began, the speed of the current was determined using the GPS by allowing the boat to float downstream with no motor activity. The current speed was found to be 0.4 mph, and from this point on data were collected only while the catamaran was being towed upstream.

To find the drag force, the catamaran was towed through the water at a constant speed which was documented along with the measurement given by the spring scale for each run. This was repeated ten times. The raw data collected during the test are displayed in Appendix A.

To evaluate the validity of the calculations, the drag force was also measured while varying the boat speed. Using the same method described above, the drag on the pontoons was observed while varying the velocity from 1 mph to 5 mph. The raw data collected during this portion of testing are included in Appendix A.

Data analysis began with a correction for the velocity of the current. Since the catamaran was always being towed upstream, the current of the river was added to the velocity of each run.

The drag force was created by towing the boat at one speed which was measured during the experiment. In order to be able to predict the drag force at different velocities

for use in a dynamic model. A coefficient of drag must be determined. Using the drag force and speed measured during the experiment the drag coefficient was determined. The force is defined using Equation 14.

$$F_D = \frac{1}{2} \cdot \rho \cdot A \cdot C_d \cdot V^2 \quad \text{(Eq. 14)}$$

In this application F_D is the drag force which was collected experimentally using a spring scale, A is the cross-sectional area of the pontoons in ft^2, C_d is the coefficient of drag, which is dimensionless, and V is the velocity at which the boat is travelling in $\frac{ft}{s}$.

Because the cross-sectional area of the boat and the drag coefficient do not change, they can be combined to form one constant that will be defined as C_{ad}. Thus, the equation is slightly simplified. It is displayed below as Equation 15.

$$F_D = \frac{1}{2} \cdot \rho \cdot C_{ad} \cdot V^2 \quad \text{(Eq. 15)}$$

Since every term in Equation 15 is known, it is possible to solve for C_{ad}. The combined coefficient of drag and cross-sectional area is used to calculate an array of drag forces by varying the velocity of the catamaran. The final equation for the coefficient of drag is Equation 16.

$$C_{ad} = \frac{2 \cdot F_D}{\rho \cdot V^2} \quad \text{(Eq. 16)}$$

Conducting the Thrust Curve Experiment

The goal of this experiment was to generate thrust curves for the two Minn Kota motors used for the 2016 Autonomous Boat. Each motor was tested individually. The test began with the motor suspended from an immobile gantry over a tank of water. The

lever that allows rotation of the motor around its mount was fixed in the open position, and the shaft of the motor was tethered to a rigid beam. An Omega LCCD-100 load cell was secured in line between the rigid beam and the motor shaft. The data sheet for the Omega LCCD-100 is in Appendix B. The distances between the pivot point and the load cell and the load cell and the propeller along the shaft were measured and recorded. As voltage is supplied to the motor, the propeller spins creating thrust, and a force can be measured by the load cell. Figure 5 is a diagram of the motor setup.

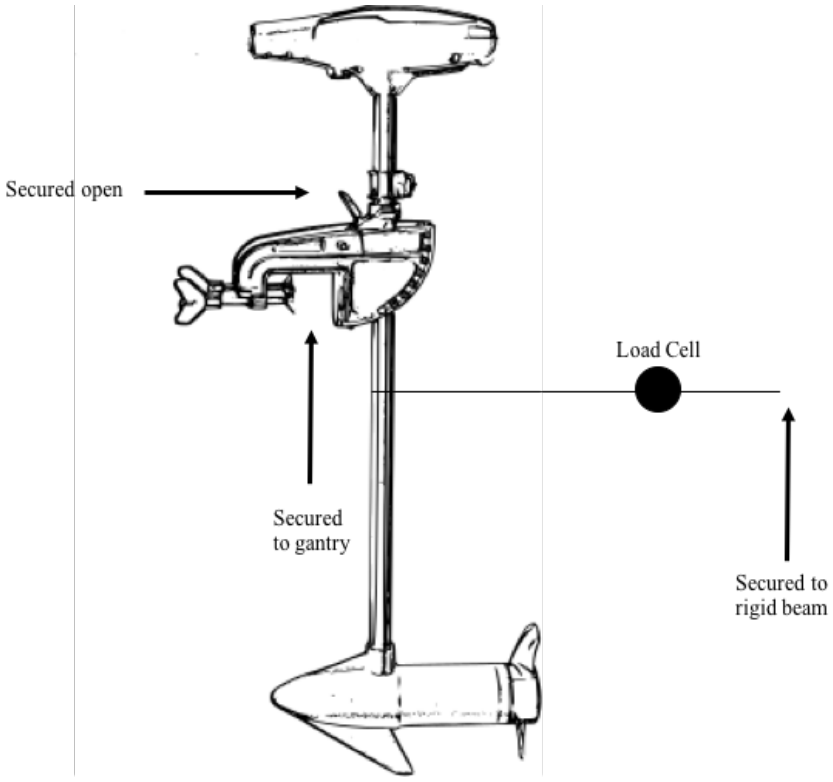

Figure 3 Minn Kota motor with trim lever secured open and load cell in line with tether

The load cell was wired to an Omega DP25-S-A display that displayed the measured force in lbf based on a voltage output from the load cell.

Each of the motors was wired though a Sabertooth 2X60 motor controller to an Arduino. When the Arduino emitted a Pulse Width Modulation (PWM) signal between 0 and 256, the motor controller converted that PWM signal to a voltage that was sent to the motor. The experiment was conducted by increasing the PWM signal from 0 to 256 in increments of 10. This signal and the corresponding force displayed on the Omega DP25-S-A were recorded for each point. The raw data collected are displayed in Appendix C

Analysis began by finding the thrust produced by the motors. The diagram below, Figure 6, helps explain why the thrust force, F_T, is not equal to the force measured in this experiment, F_l.

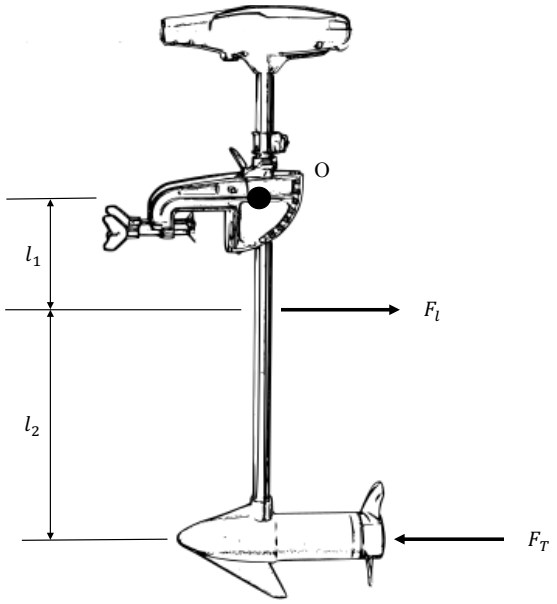

Figure 4 Free body diagram of trolling motor during test

This is a static system, so the thrust for each motor can be found by summing the moments about point O and setting them equal to zero. An example calculation is displayed below.

$$\circlearrowleft M_O = F_l l_1 - F_t l_2 \qquad \text{(Eq. 17)}$$

$$0 = F_l l_1 - F_t l_2$$

From here, the thrust can be isolated and solved for.

$$F_t = \frac{l_1}{l_2} F_l \qquad \text{(Eq. 18)}$$

Equation 18 was used on the raw data, and the resulting forces for each motor were graphed against the PWM signals emitted by the Arduino.

Constructing the Model

With the equations of motion derived and the relationships between thrust and PWM signal and drag and velocity known, the final model could be completed. To do this, each of the equations of motion were rearranged to isolate the velocity assuming no acceleration. Equation 19 and 20 are the results.

$$V = \sqrt{-\frac{2F}{\frac{1}{2} \cdot \rho \cdot C_{Df} A}} \qquad \text{Eq. 19}$$

$$\omega = \sqrt{\frac{\left(-F_2 \cdot \frac{b}{2} + F_1 \cdot \frac{b}{2}\right)}{\frac{b}{16} \cdot \rho \cdot C_{Dr} A}} \qquad \text{Eq. 20}$$

In the equations above, V is the linear velocity, and ω is the rotational velocity of the catamaran.

A program was written in Matlab_R2015b to generate graphs of the linear and rotational velocities given the full range of PWM signals (0 to 256). The full program has been included in Appendix D.

Results

While the dynamic model was the focus of study a number of outcomes resulted from the thesis. The equations of motion as well as drag and thrust curves were intermediate results which are of general utility in the design of the autonomous boat. The results section is organized in the same manner as the methods and analysis.

Equations of Motion

The equations that describe the motion of this catamaran were successfully derived. The linear equation of motion is $ma = \frac{1}{2} \cdot \rho \cdot \dot{x}^2 C_{Df} A + 2F$, and the rotational is $I\alpha = \frac{b}{16} \cdot \rho \cdot \dot{\theta}^2 C_{Dr} A + F_2 \cdot \frac{b}{2} - F_1 \cdot \frac{b}{2}$.

Drag

The combined drag coefficient and area term, C_{ad} was found to be $0.01946 ft^2$. Given a target velocity of 5 mph, this would induce a drag force of 40 lbf.

Two drag curves were generated for display and can be seen in Figure 7 and 8 below. Figure 8 displays the predicted drag curve which was calculated using Equation 15. This curve displays calculated drag data well beyond the desired speed of the catamaran.

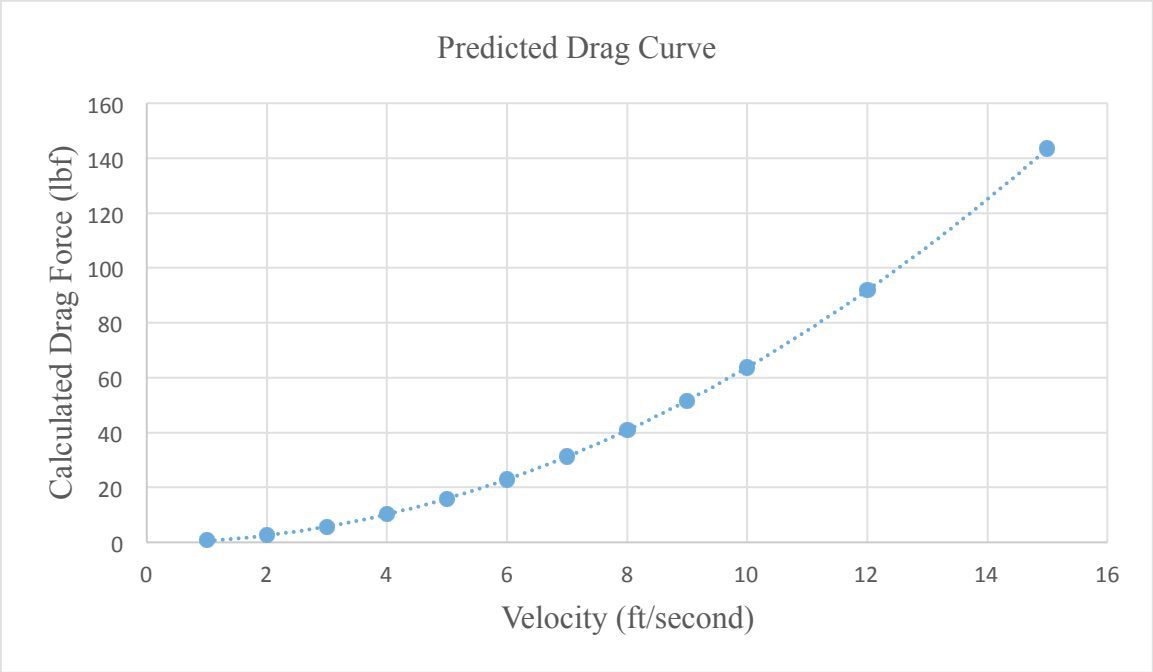

Figure 5 Predicted drag curve depicting the drag calculated using Equation 15 for each velocity

The second curve, shown in Figure 9, displays the measured data collected during the experiment.

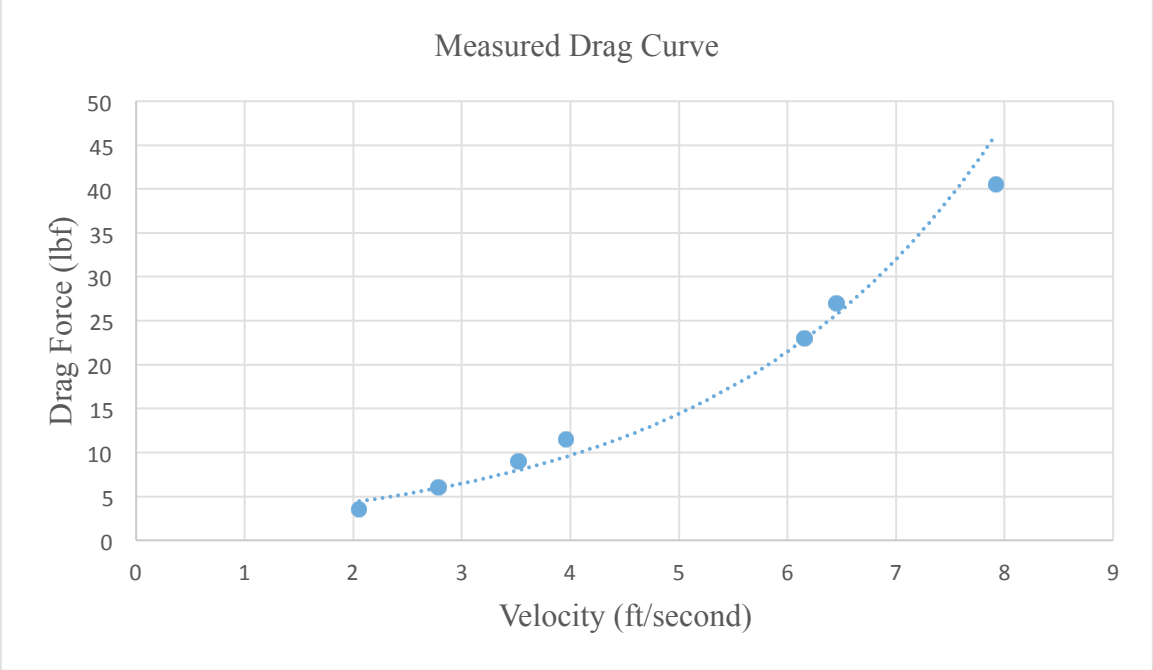

Figure 6 Drag curve using measured data

The predicted and measured data differ by about 10%. See Appendix A for complete data and analysis.

The desired result of this experiment for use in the dynamic model, an array of predicted drag forces produced by varying the velocity of the catamaran, was also generated. It is displayed below in Table 1.

Table 1 Predicted drag data

Velocity (ft/s)	Calculated drag (lbf)
1	0.64
2	2.55
3	5.74
4	10.20
5	15.94
6	22.96
7	31.25
8	40.81
9	51.65
10	63.77
12	91.83
15	143.48

Thrust Curves

The results of the thrust experiments can be displayed graphically and in tabulated values. The graphs of the forward thrust curves for each motor, corresponding to PWM signals 1 to 100, are included below as Figures 9 and 10.

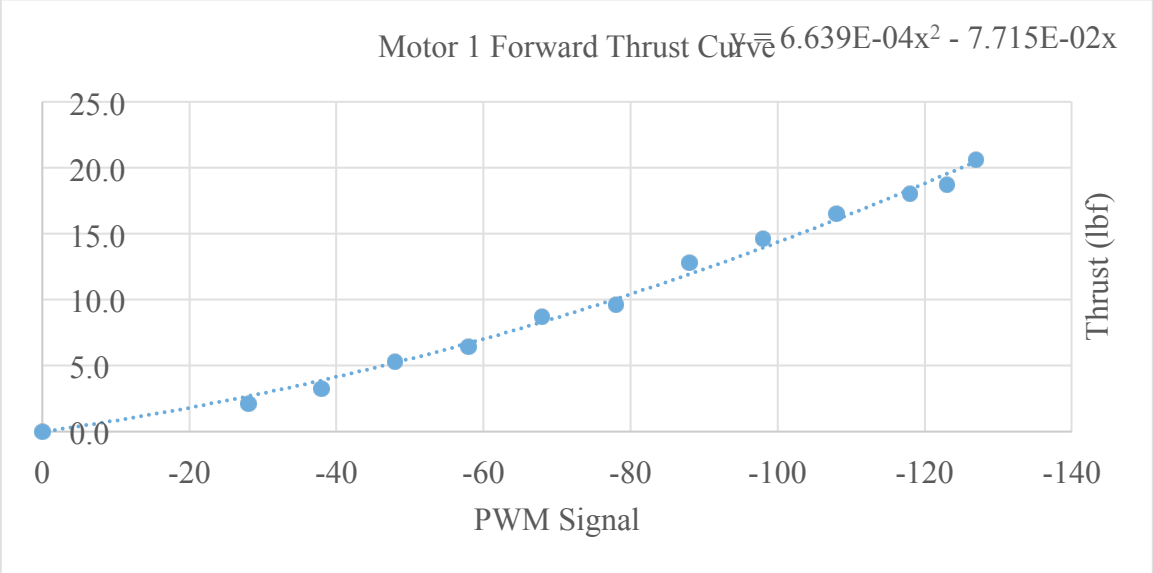

Figure 7 Forward thrust curve for motor 1

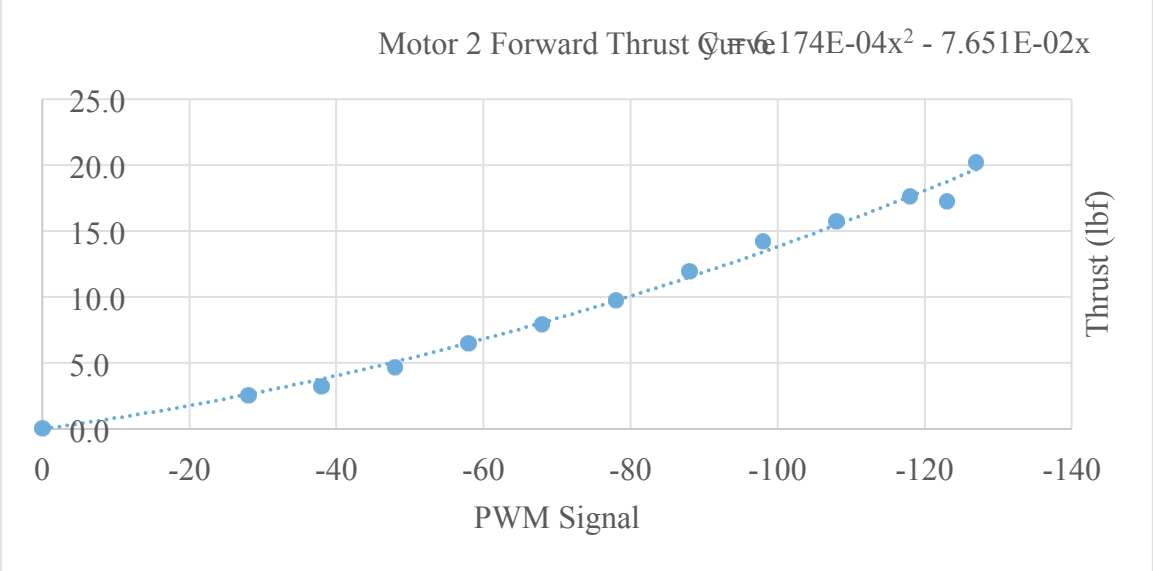

Figure 8 Forward thrust curve for motor 2

The graphs of the reverse thrust curves for each motor, corresponding to PWM signals 170 to 255, are included below as Figures 11 and 12.

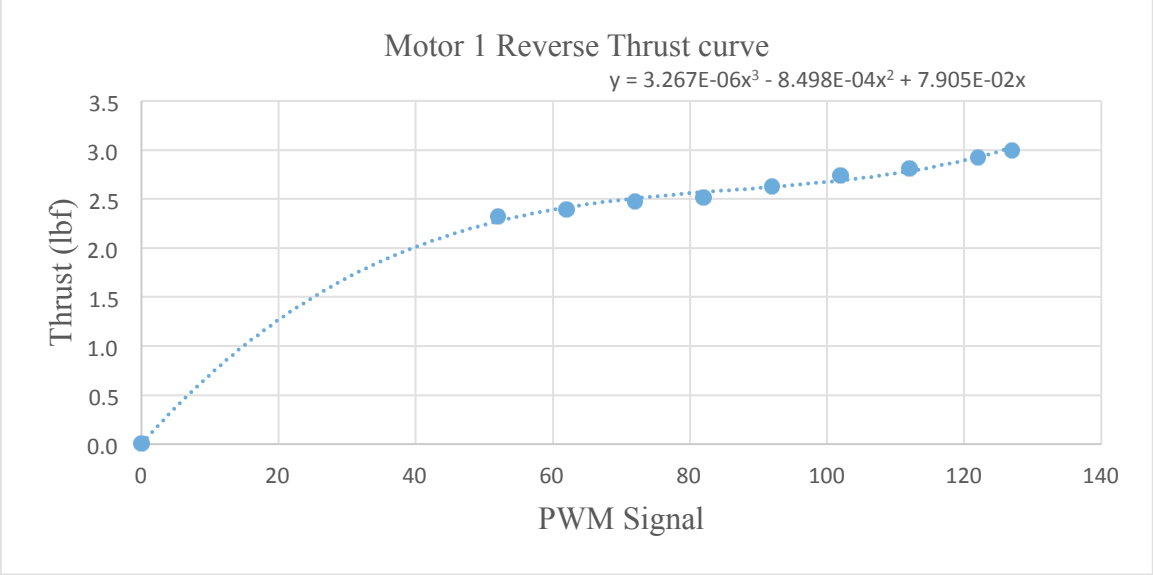

Figure 9 Reverse thrust curve for motor 1

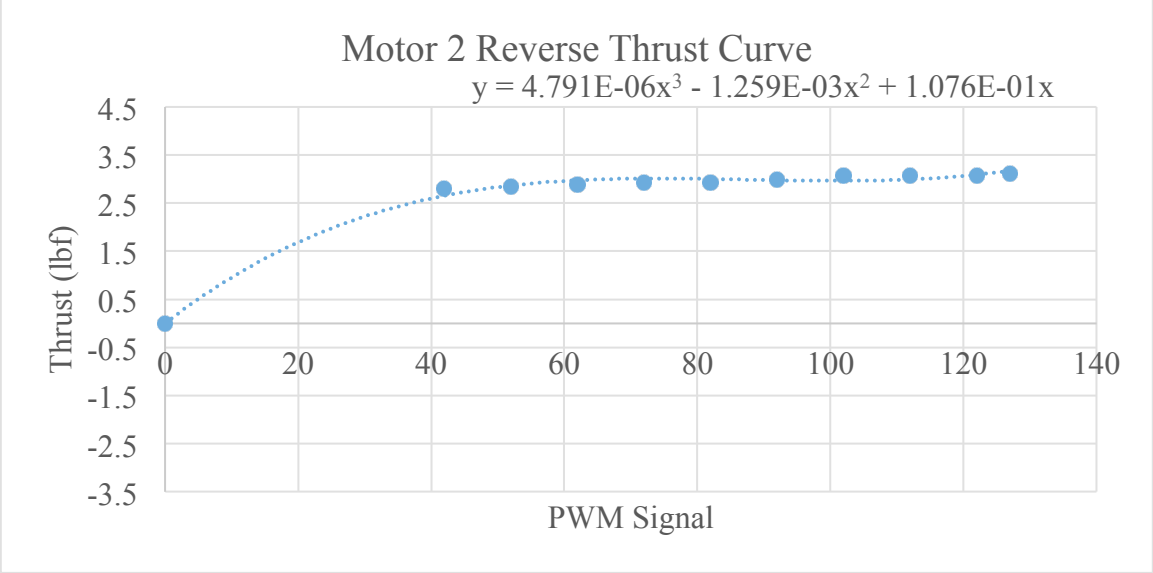

Figure 10 Reverse thrust curve for motor 2

Tabulated values were also needed to complete the model. A table of data was corrected and displayed below in Table 2.

Table 2 Experimental thrust curve data

Motor 1			Motor 2	
PWM Signal	Corrected Thrust (lbf)		PWM Signal	Corrected Thrust (lbf)
255	3		255	3.1125
250	2.925		250	3.075
240	2.8125		240	3.075
230	2.7375		230	3.075
220	2.625		220	3
210	2.5125		210	2.925
200	2.475		200	2.925
190	2.4		190	2.8875
180	2.325		180	2.85
100	2.1		100	2.5875
90	3.225		90	3.225
80	5.2875		80	4.6875
70	6.45		70	6.4875
60	8.7		60	7.9875
50	9.6		50	9.7875
40	12.75		40	11.9625
30	14.625		30	14.25
20	16.5		20	15.75
10	18		10	17.625
5	18.75		5	17.2875
1	20.625		1	20.25

Model

A model was successfully completed. The resulting model utilizes the equations of motion and the thrust and drag coefficient which was calculated for this purpose. That model has been used to predict the linear and rotational velocity with different PWM signal inputs. The results can be seen graphically in Figures 13 and 14 below.

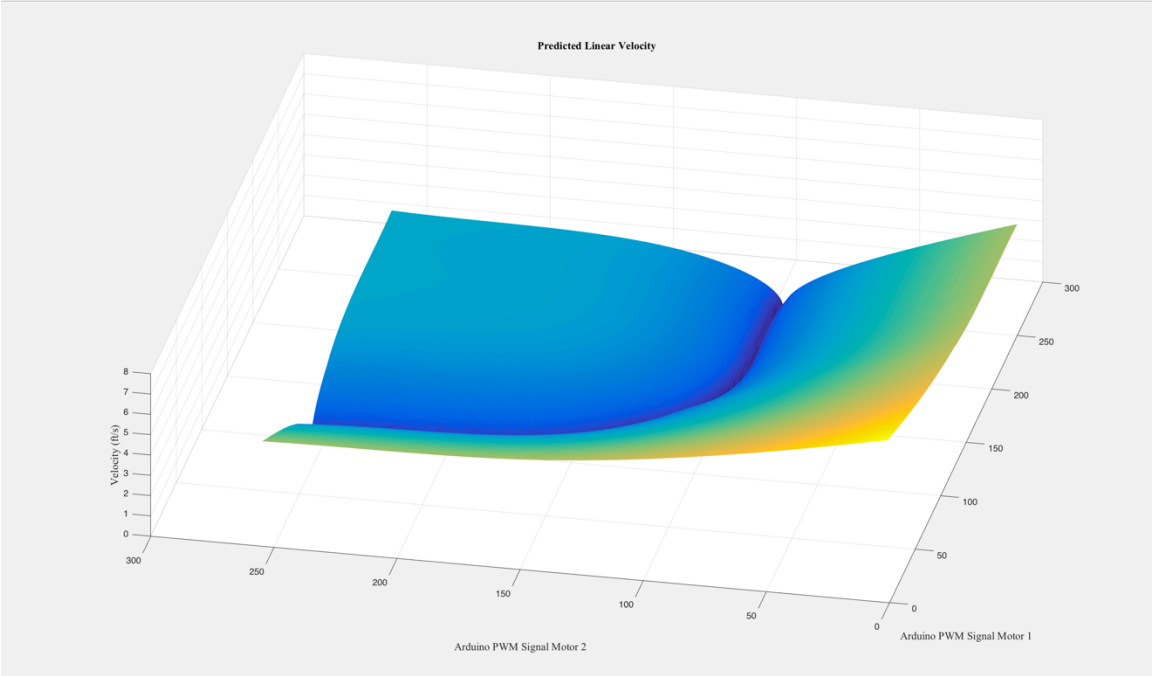

Figure 11 Predicted linear velocity of the catamaran

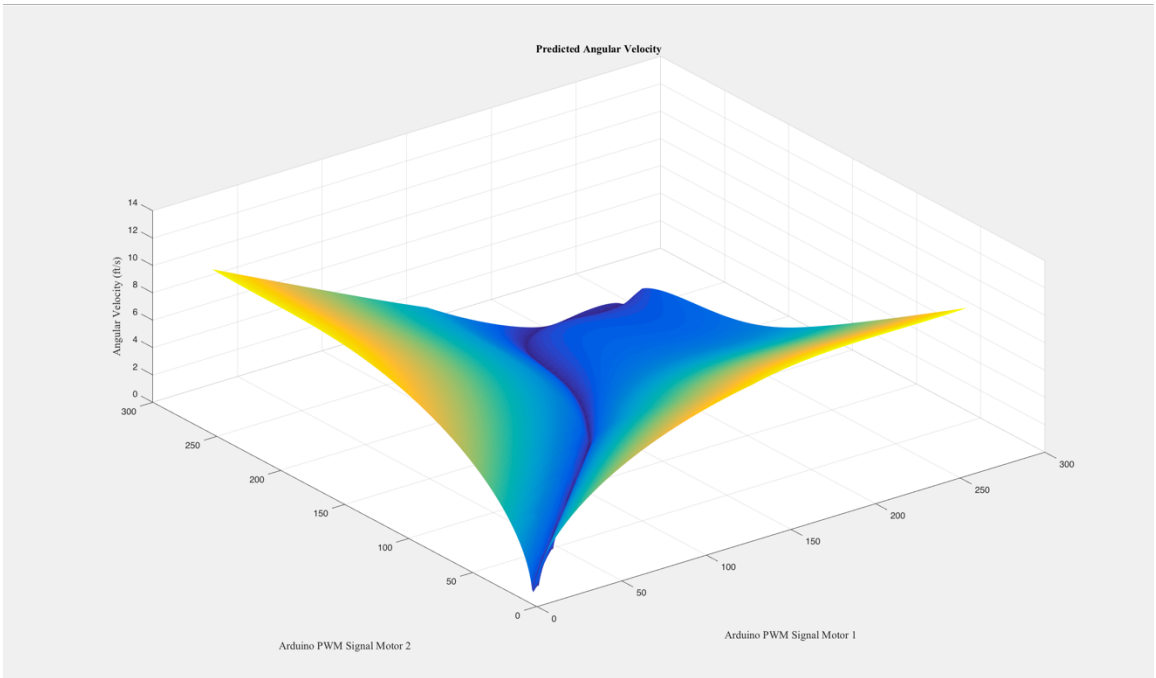

Figure 12 Predicted angular velocity of the catamaran

Each of the resulting graphs has three axes. The PWM signals for each of the motors are displayed in two of them, and the linear or angular velocity resulting from the pair is the third axis.

The linear velocity graph is Figure 13. PWM signals of zero to both motors produces a peak velocity represented by the yellow portion of the graph. This represents forward motion. PWM signals of 255 to both motors produces another region of high velocity. This represents reverse motion. The low region on the graph is the area where the motors are working against each other and forward and reverse thrust are matched.

The angular velocity graph (Figure 14) is slightly less intuitive. On either side is a region of intense yellow, this is high velocity. It represents a situation when one motor is producing forward thrust and the other is producing negative thrust. The low region on the graph is the area where the motion is completely linear, so the thrust of the motors is equal. There is a pronounced curve in this region which is present because the thrust curves of the engines are not identical.

Conclusions and Future Work

The objective of this thesis was to create a dynamic model, and that objective was met. A system of equations was derived to predict the motion of the 2016 Autonomous Boat Team's catamaran, and the drag coefficient and thrust force were determined so the model could be used.

The equations of motion are $ma = \frac{1}{2} \cdot \rho \cdot \dot{x}^2 C_{Df} A + 2F$ and $I\alpha = \frac{b}{16} \cdot \rho \cdot \dot{\theta}^2 C_{Dr} A + F_2 \cdot \frac{b}{2} - F_1 \cdot \frac{b}{2}$. The combined drag and area coefficient was found, and the

drag forces calculated using it were found to have 10.6% error from the measured values. Thrust curves were generated, and they convey the inability of the engines to produce negative thrust. This means that the boat cannot travel backwards and cannot turn effectively with the current propeller design.

The results of this thesis clearly show opportunities for future work on both the model and the autonomous catamaran. The next step for the catamaran is to add two more motors mounted in the opposite direction of the first two. With four motors, the catamaran would be nimbler. The thrust curves for the two additional motors should then be generated, and the two extra forces should be added to the model.

Though there are many improvements left to be made on this model, I do not want to understate its merits or undervalue the results that have been produced for the completion of this project. The thrust curves allowed for the thrust of the motors to be matched, which is crucial for in making the boat travel forward. The drag curve will be of significant use for sizing new motors, and with a few modifications to include a third axis as well as wave and current, hopefully the entire model will prove useful to help the 2017 Autonomous Boat Team make a seaworthy prototype.

Bibliography

1. *Hydroelectric Power: Managing Water In The West*. 1st ed. 2005. Web. 8 Feb. 2016.

2. "Circulation » Gulf Of Maine Census". *Gulfofmaine-census.org*. N.p., 2016. Web. 13 Mar. 2016.

3. "Cobscook Bay: An Extraordinary Estuary With “Boiling Tides” :: NOAA Fisheries". *Greateratlantic.fisheries.noaa.gov*. N.p., 2016. Web. 14 Mar. 2016.

4. Newton, Isaac, William Thomson Kelvin, and Hugh Blackburn. *Sir Isaac Newton's Principia*. Glasgow: J. Maclehose, 1871. Print.

5. Ross, Andrew. "A Rudimentary History Of Dynamics". *MIC* 30.4 (2009): 223-235. Web.

6. Williams, James H. *Fundamentals Of Applied Dynamics*. New York: J. Wiley, 1996. Print.

7. Munson, Bruce Roy, Donald F Young, and T. H Okiishi. *Fundamentals Of Fluid Mechanics*. New York: Wiley, 1994. Print.

APPENDIX A

Table 3 Measured velocity and measured and calculated drag

Velocity (ft/sec)	Calculated drag (lbf)	Measured Drag (lbf)	Measured-Calculated	Error
2.053	2.688	3.5	0.811	0.231
2.786	4.951	6	1.048	0.174
3.52	7.901	9	1.098	0.122
3.96	10	11.5	1.5	0.130
6.16	24.197	23	-1.197	0.052
6.453	26.556	27	0.443	0.016
7.92	40	40.5	0.5	0.012
			TOTAL	0.105

APPENDIX B

O M E G A E N G I N E E R I N G I N C.

LOAD CELL
FINAL CALIBRATION

0.00 - 100.00 LBS
Excitation 10.000 Vdc

Job: WHM5137 Serial: 322660
Model: LCCD-100 Tested By: WF
Date: 12/1/2015 Temperature Range: +0 to +150 F
Calibrated: 0.00 - 100.00 LBS Specfile: LCCD

Force LBS	Unit Data mVdc	Normalized Data
0.00	- 0.103	0.000
50.00	14.883	14.986
100.00	29.836	29.939
50.00	14.882	14.985
0.00	- 0.104	- 0.001

Balance	- 0.103	mVdc	
Sensitivity	29.939	mVdc	
In Resist	470.80	Ohms	
Out Resist	351.60	Ohms	
59K Shunt	14.832	mVdc	Change at 0.00 LBS (-INPUT to -OUTPUT)

Calibration Factors:
Sensitivity = 2.994 mV/V 59K Shunt = 1.483 mV/V

ELECTRICAL LEAKAGE: PASS
ELECTRICAL WIRING/CONNECTOR: RED = +EXCITATION
BLACK = -EXCITATION
GREEN = +OUTPUT
WHITE = -OUTPUT

This Calibration was performed using Instruments and Standards that are traceable to the United States National Institute of Standards Technology.

S/N	Description	Range	Reference	Cal Cert
	10001b Reference STD	0 - 100.00 LBS	C-2692	C-2692
3146A40859	HP34401A DMM UUT	Unit Under Test	C-2412	C-2412

Q.A. Representative : *William Flecter* Date: 12/1/2015

This transducer is tested to & meets published specifications. After final calibration our products are stored in a controlled stock room & considered in bonded storage. Depending on environment & severity of use factory calibration is recommended every one to three years after initial service installation date.
COMMENTS: FINAL TEST.

Omega Engineering Inc., One Omega Drive, Stamford, CT 06907
http://www.omega.com email: info@omega.com phone (800) 826-6342

APPENDIX C

Table 4 Raw and processed data collected during experiment

	Motor 1		Motor 2	
PWM Signal	Raw Force (lbf)	Thrust (lbf)	Raw Force (lbf)	Thrust (lbf)
255	8	3.0	8.3	3.1
250	7.8	2.9	8.2	3.1
240	7.5	2.8	8.2	3.1
230	7.3	2.7	8.2	3.1
220	7	2.6	8	3.0
210	6.7	2.5	7.8	2.9
200	6.6	2.5	7.8	2.9
190	6.4	2.4	7.7	2.9
180	6.2	2.3	7.6	2.9
100	5.6	2.1	6.9	2.6
90	8.6	3.2	8.6	3.2
80	14.1	5.3	12.5	4.7
70	17.2	6.5	17.3	6.5
60	23.2	8.7	21.3	8.0
50	25.6	9.6	26.1	9.8
40	34	12.8	31.9	12.0
30	39	14.6	38	14.3
20	44	16.5	42	15.8
10	48	18.0	47	17.6
5	50	18.8	46.1	17.3
1	55	20.6	54	20.3

APPENDIX D

```
%*************************************************************************
%*************************************************************************
%***************     Dynamic Model of a Catamaran     ********************
%***************         By Tamara Thomson            ********************
%***************         Revised May 5, 2016          ********************
%*************************************************************************
%*************************************************************************

clc, clear all, close all

rho=65.55;
CdA=.01946;
step = 1;
b=8.5

for PWM1=1:255/step;
   for PWM2=1:255/step;

 if (PWM1<=128/step);
   F1 = 6.639e-4*(PWM1-128)^2-7.715e-2*(PWM1-128);

 end

  if(PWM1 > 128/step)
     F1 = -1*(3.267e-6*(PWM1-128)^3-8.498e-4*(PWM1-128)^2+7.905e-2*(PWM1-128));
 end

if (PWM2 <= 128/step);
   F2 = 6.174e-4*(PWM2-128)^2-7.651e-2*(PWM2-128);
end

 if(PWM2 > 128/step)
     F2 = -1*(4.791e-6*(PWM2-128)^3-1.259e-3*(PWM2-128)^2+1.076e-1*(PWM2-128))
 end
V(PWM1,PWM2) = (abs(F1+F2)/(.5*rho*CdA)).^(1/2);  %no acceleration
w(PWM1,PWM2) = (abs(-F2*b/2+F1*b/2)/(b/16*rho*CdA)).^(1/2);   %no acceleration
   end
end

V
figure
hSurf = surf(V,'EdgeColor','none','LineStyle','none','FaceLighting','phong');
figure
hSurf = surf(w,'EdgeColor','none','LineStyle','none','FaceLighting','phong');
```

Author's Biography

Tamara R. Thomson was born in Harlingen, Texas on December 12, 1993. She attended Woodland High School in Baileyville, Maine where she graduated at the top of her class in 2012. Tamara will graduate from the University of Maine in May of 2016 with a degree in mechanical engineering and a minor in mathematics. She is a member of Pi Tau Sigma Honor Society and chapter Vice President of the Society of Women Engineers.

After graduation, Tamara plans to backpack the Camino de Santiago before beginning a career with General Motors in July of 2016. Within the first few years of beginning work, she plans to pursue an advanced degree in engineering.